*Progress In Electromagnetics Research, Vol. 135, 677–694, 2013*

# EVALUATION OF ELECTROMAGNETIC FIELDS DUE TO INCLINED LIGHTNING CHANNEL IN PRESENCE OF GROUND REFLECTION

**Mahdi Izadi[1, 2, *], Mohd Z. A. Ab Kadir[1], and Maryam Hajikhani[1]**

[1]Centre for Electromagnetic and Lightning Protection Research (CELP), Faculty of Engineering, Universiti Putra Malaysia, UPM, Serdang 43400, Selangor, Malaysia

[2]Department of Electrical, Firoozkooh Branch, Islamic Azad University, Firoozkooh, Iran

**Abstract**—In this paper, analytical field expressions are proposed to determine the electromagnetic fields due to an inclined lightning channel in the presence of a ground reflection at the striking point. The proposed method can support different current functions and models directly in the time domain without the need to apply any extra conversions. A set of measured electromagnetic fields associated with an inclined lightning channel from a triggered lightning experiment is used to evaluate the proposed field expressions. The results indicate that the peak of the electromagnetic fields is dependent on the channel angle, the observation point angle as well as the value of the ground reflection factor due to the difference between channel and ground impedances. Likewise, the effect of the channel parameters and the ground reflection on the values of the electromagnetic fields is considered and the results are discussed accordingly.

## 1. INTRODUCTION

The electromagnetic fields associated with a lightning channel can be considered as a source of lightning induced voltage on power lines whereby they are strongly dependent on the shape of lightning channel, lightning current parameters at different heights along the lightning channel and a number of geometrical parameters [1–7]. On the other hand, the ground reflection due to the difference between return stroke

*Received 25 November 2012, Accepted 26 December 2012, Scheduled 8 January 2013*
* Corresponding author: Mahdi Izadi (aryaphase@yahoo.com).

channel impedance and the ground impedance at connection point (channel base) can have an effect on the shapes of the lightning return stroke currents at different heights along a lightning channel as well as the lightning induced electromagnetic fields. However, in reality a lightning strike to the surface of the ground has different channel angles with respect to the vertical axis that are usually higher than zero for at least the first hundred meters of the channel and the shape of the channel can also have an effect on the values of the lightning electromagnetic fields [6, 8, 9]. In this paper, a set of electromagnetic field expressions are proposed to include the inclined channels as well as the ground reflection at the channel base directly in the time domain without the need to apply any extra conversions. The basic assumptions in this study are listed as follows:

1- The surface of the ground is assumed to be flat.
2- The ground conductivity is assumed to be perfect.
3- The effect of lightning branches is ignored.

## 2. RETURN STROKE CURRENT

The return stroke current along a lightning channel can be considered in two areas, i.e., the channel base and at different heights above the surface of the ground whereby they can be modelled by current functions and current models, respectively [10, 11]. In this paper, the sum of two Heidler functions and the general form of the engineering current model are used as expressed by Equations (1) and (2), respectively [10–16]. It should be mentioned that the ground reflection is ignored in Equation (2).

$$i\left(0,t\right)=\left[\frac{i_{01}}{\eta_1}\frac{\left(\frac{t}{\tau_{11}}\right)^{n_1}}{1+\left(\frac{t}{\tau_{11}}\right)^{n_1}}\exp\left(\frac{-t}{\tau_{12}}\right)+\frac{i_{02}}{\eta_2}\frac{\left(\frac{t}{\tau_{21}}\right)^{n_2}}{1+\left(\frac{t}{\tau_{21}}\right)^{n_2}}\exp\left(\frac{-t}{\tau_{22}}\right)\right] \quad (1)$$

$$i\left(z',t\right)=i\left(0,t-\frac{z'}{v}\right)P\left(z'\right)U\left(t-\frac{z'}{v_f}\right) \quad (2)$$

where:

$i(0, t)$ is the channel base current,

$t$ is the time step,

$i_{01}/i_{02}$ is the current amplitude of first/second Heidler function in Equation (1),

$\tau_{11}/\tau_{12}$ is the front time constant of first/second Heidler function in Equation (1),

$\tau_{21}/\tau_{22}$ is the decay-time constant in first/second Heidler function in Equation (1),

$n_1$ and $n_2$ are exponent ($2 \sim 10$),

$$\eta_1 = \exp\left[-\left(\tau_{11}/\tau_{12}\right)\left(n_1\frac{\tau_{12}}{\tau_{11}}\right)^{\frac{1}{n_1}}\right],$$

$$\eta_2 = \exp\left[-\left(\tau_{21}/\tau_{22}\right)\left(n_2\frac{\tau_{22}}{\tau_{21}}\right)^{\frac{1}{n_2}}\right],$$

$z'$ is temporary charge height along channel,

$v$ is return stroke current velocity along channel,

$v_f$ is return stroke current velocity along channel,

$U(t-\frac{z'}{v_f})$ is Heaviside function.

Equation (2) shows that the current wave shapes at different heights above the surface of the ground are dependent on the channel base current function and an attenuation height dependent function whereby a number of current models can be based on the values of the $P(z')$ term and $v$ in Equation (2). In this paper, the attenuation height dependent factor is set for the MTLE (Modified Transmission Line with Exponential decay model) current model with an attenuation function $P(z') = \exp(-z'/\lambda)$ where the value of $\lambda$ is constant and is typically between 1–2 km [16–18]. It should be noted that the return stroke velocity is usually assumed to be a constant value between $c/3$ to $2c/3$ where $c$ is the speed of light in free space [16, 19]. By taking account of the effect of the ground reflection on the shape of the return stroke current, Equation (2) can be converted into Equation (3) whereby the reflected current is propagated along the lightning channel at the speed of light in free space and the original reflected currents are controlled by the return stroke front, whereas the reflected current (the second term of Equation (3)) is strongly dependent on the ground reflection factor [20]. It is noted that the ground reflection is due to the difference between the channel and the ground impedances at connection point (at the channel base) which can be expressed by $\rho_g = \frac{z_{ch}-z_g}{z_{ch}+z_g}$. Therefore, the additional current term (the second term of Equation (3)) will have an effect on the values of the lightning electromagnetic fields as well as the original current term (the first term of Equation (3)) that is considered in the next section.

$$i_{gr}\left(z',t\right) = \left[P\left(z'\right)i\left(0,t-\frac{z'}{v}\right) + \rho_g i\left(0,t-\frac{z'}{c}\right)\right]U\left(t-\frac{z'}{v_f}\right) \quad (3)$$

where:

$\rho_g$ is ground reflection coefficient equal to $\frac{z_{ch}-z_g}{z_{ch}+z_g}$,

$z_{ch}$ is the surge impedance of return stroke channel,

$z_g$ is the ground impedance,

$i_{gr}(z', t)$ is the return stoke current at different heights along channel in presence of ground reflection factor.

## 3. LIGHTNING ELECTROMAGNETIC FIELDS

The lightning electromagnetic fields associated with an inclined lightning channel in the presence of a ground reflection are considered in this section and the geometry of the problem is shown in Figure 1 with the current model based on Equation (3). Therefore, by

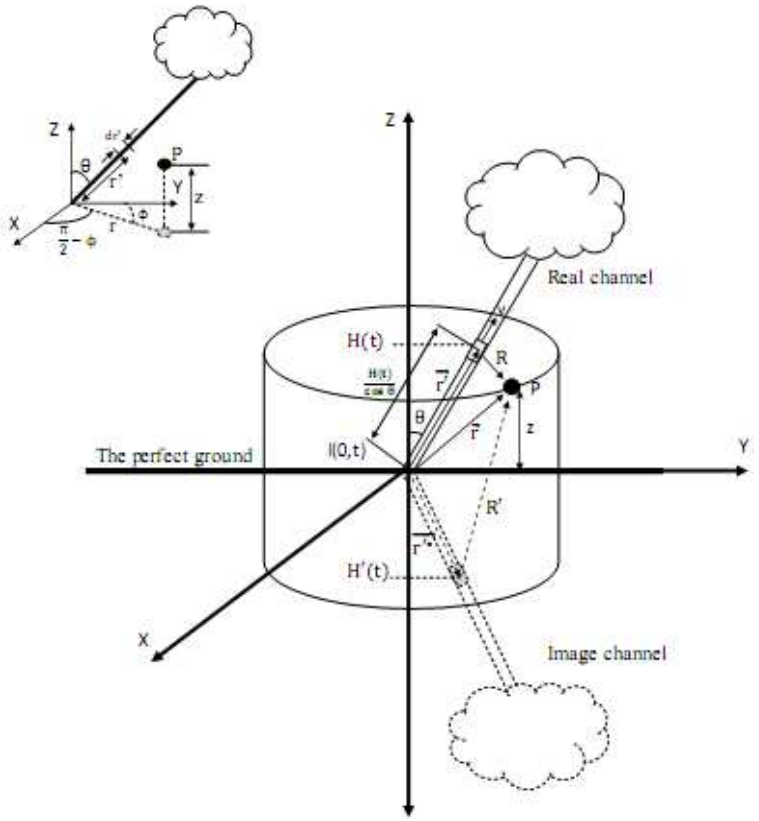


**Figure 1.** Geometry of problem [8].

assuming an observation point above the surface of the ground the electromagnetic field expressions are expressed by Equations (4) to (6) and Maxwell's equations [21, 22], Lorentz gauge [23] and also the Dipole [8, 9, 24], FDTD [25–27] and Trapezoid [26] methods are applied

$$\begin{aligned}
&\vec{B}_{\varphi}\left(r,z,\phi,\theta,t_n\right)\\
&=-\sin\left(\frac{\pi}{2}-\phi\right)\left[\sum_{i=1}^{n}\sum_{m=1}^{k+1}\left\{a_m F_{i,1}\left(x,y,z,\theta,t=t_n,r'=h_{m,i}\right)\right.\right.\\
&\left.\left.-a'_m F_{i,1}\left(x,y,z,\theta,t=t_n,r'=h'_{m,i}\right)\right\}\right]+\cos\left(\frac{\pi}{2}-\phi\right)\\
&\times\left[\sum_{i=1}^{n}\sum_{m=1}^{k+1}\left\{a_m F_{i,2}\left(x,y,z,\theta,t=t_n,r'=h_{m,i}\right)\right.\right.\\
&\left.\left.-a'_m F_{i,2}\left(x,y,z,\theta,t=t_n,r'=h'_{m,i}\right)\right\}\right] \qquad (4)\\
&\vec{E}_{r}\left(r,z,\phi,\theta,t_n\right)\\
&=\Delta t\times\left\{\cos\left(\frac{\pi}{2}-\phi\right)\left[\sum_{i=1}^{n}\sum_{m=1}^{k+1}\left\{a_m F_{i,3}\left(x,y,z,\theta,t=t_{n-1},r'=h_{m,i}\right)\right.\right.\right.\\
&\left.\left.\left.-a'_m F_{i,3}\left(x,y,z,\theta,t=t_{n-1},r'=h'_{m,i}\right)\right\}\right.\right.\\
&\left.\left.+\sum_{i=1}^{n}\sum_{m=1}^{k+1}\left\{a_m F_{i,3}\left(x,y,z,\theta,t=t_n,r'=h_{m,i}\right)\right.\right.\right.\\
&\left.\left.\left.-a'_m F_{i,3}\left(x,y,z,\theta,t=t_n,r'=h'_{m,i}\right)\right\}\right]+\sin\left(\frac{\pi}{2}-\phi\right)\\
&\times\left[\sum_{i=1}^{n}\sum_{m=1}^{k+1}\left\{a_m F_{i,4}\left(x,y,z,\theta,t=t_{n-1},r'=h_{m,i}\right)\right.\right.\\
&\left.\left.-a'_m F_{i,4}\left(x,y,z,\theta,t=t_{n-1},r'=h'_{m,i}\right)\right\}\right.\\
&\left.+\sum_{i=1}^{n}\sum_{m=1}^{k+1}\left\{a_m F_{i,4}\left(x,y,z,\theta,t=t_n,r'=h_{m,i}\right)\right.\right.\\
&\left.\left.-a'_m F_{i,4}\left(x,y,z,\theta,t=t_n,r'=h'_{m,i}\right)\right\}\right] \qquad (5)\\
&\vec{E}_{z}\left(r,z,\phi,\theta,t_n\right)\\
&=\Delta t\times\left[\sum_{i=1}^{n}\sum_{m=1}^{k+1}\left\{a_m F_{i,5}\left(x,y,z,\theta,t=t_{n-1},r'=h_{m,i}\right)\right.\right.\\
&\left.\left.-a'_m F_{i,5}\left(x,y,z,\theta,t=t_{n-1},r'=h'_{m,i}\right)\right\}\right.\\
&\left.+\sum_{i=1}^{n}\sum_{m=1}^{k+1}\left\{a_m F_{i,5}\left(x,y,z,\theta,t=t_n,r'=h_{m,i}\right)\right.\right.\\
&\left.\left.-a'_m F_{i,5}\left(x,y,z,\theta,t=t_n,r'=h'_{m,i}\right)\right\}\right] \qquad (6)
\end{aligned}$$

where:

$\vec{E}_r(r,\, z,\, \phi,\, \theta,\, t_n)$ is the horizontal electric field due to inclined lightning channel,

$\vec{E}_z(x,\, y,\, z,\, \theta,\, t,\, r')$ is the vertical electric field due to inclined lightning channel,

$\vec{B}_\varphi(r,\, z,\, \phi,\, \theta,\, t_n)$ is the magnetic flux density in $\varphi$-direction due to inclined lightning channel,

$r$ is radial distance from channel base to image of observation point on the ground surface ($r = \sqrt{x^2 + y^2}$),

$r'$ is the temporary channel length along the lightning channel,

$\theta$ is the angle between lightning channel and $z$ axis (the channel angle),

$\phi$ is the angle between $y$ axis and $\vec{r}$ (observation point angle),

$x$ is the position of observation point at $x$ axis ($x = r\sin\phi$),

$y$ is the position of observation point at $y$ axis ($y = r\cos\phi$),

$z$ is observation point height from ground surface,

$\phi = \arccos\left(\frac{y}{\sqrt{x^2+y^2}}\right)$,

$A_1\,(r') = 2\,(z - r'\cos\theta)$,

$A_2\,(r') = 2\,(y - r'\sin\theta)$,

$\Delta t$ is the time step,

$n$ is the number of time steps,

$$t_n = \frac{\sqrt{r^2 + z^2}}{c} + (n-1)\Delta t \quad n = 1, 2, \ldots n_{\max}$$

$$F_{i,1}(x, y, z, \theta, t, r')$$

$$= 10^{-7}\left\{-\cos\theta\left[\frac{y - r'\sin\theta}{cR\,(r')^2}\frac{\partial i_{gr}\left(r', t - \frac{R(r')}{c}\right)}{\partial t} + \frac{y - r'\sin\theta}{R\,(r')^3} i_{gr}\left(r', t - \frac{R\,(r')}{c}\right)\right]\right.$$

$$\left. + \sin\theta\left[\frac{z - r'\cos\theta}{cR\,(r')^2}\frac{\partial i_{gr}\left(r', t - \frac{R(r')}{c}\right)}{\partial t} + \frac{z - r'\cos\theta}{R\,(r')^3} i_{gr}\left(r', t - \frac{R\,(r')}{c}\right)\right]\right\}$$

$$F_{i,2}(x, y, z, \theta, t, r')$$

$$= 10^{-7} \times \cos\theta\left\{\frac{x}{cR\,(r')^2}\frac{\partial i_{gr}\left(r', t - \frac{R(r')}{c}\right)}{\partial t} + \frac{x}{R\,(r')^3} i_{gr}\left(r', t - \frac{R\,(r')}{c}\right)\right\}$$

$$
\begin{aligned}
&F_{i,3}\left(x,y,z,\theta,t,r'\right)\\
&=\frac{1}{4\pi\varepsilon_0}\times\left[\frac{3x\sin\theta(y-r'\sin\theta)}{R\left(r'\right)^5}\times i_{gr}\left(r',t-\frac{R\left(r'\right)}{c}\right)+\frac{3x\sin\theta(y-r'\sin\theta)}{cR\left(r'\right)^4}\right.\\
&\times\frac{\partial i_{gr}\left(r',t-\frac{R(r')}{c}\right)}{\partial t}+\frac{x\sin\theta(y-r'\sin\theta)}{c^2R\left(r'\right)^3}\times\frac{\partial i_{gr}^2\left(r',t-\frac{R(r')}{c}\right)}{\partial t^2}\\
&+\frac{3x\cos\theta(z-r'\cos\theta)}{R\left(r'\right)^5}\times i_{gr}\left(r',t-\frac{R\left(r'\right)}{c}\right)+\frac{3x\cos\theta(z-r'\cos\theta)}{cR\left(r'\right)^4}\\
&\left.\times\frac{\partial i_{gr}\left(r',t-\frac{R(r')}{c}\right)}{\partial t}+\frac{x\cos\theta(z-r'\cos\theta)}{c^2R\left(r'\right)^3}\times\frac{\partial i_{gr}^2\left(r',t-\frac{R(r')}{c}\right)}{\partial t^2}\right]\\
&F_{i,4}\left(x,y,z,\theta,t,r'\right)\\
&=\frac{1}{4\pi\varepsilon_0}\left[\left\{\frac{3}{4}\times\frac{A_1(r')A_2(r')\cos\theta-A_1(r')^2\sin\theta}{R(r')^5}+\frac{\sin\theta}{R(r')^3}\right\}\times i_{gr}\left(r',t-\frac{R(r')}{c}\right)\right.\\
&-\frac{1}{2}\left\{\left(\frac{-A_2\left(r'\right)\cos\theta+A_1\left(r'\right)\sin\theta}{2cR\left(r'\right)^4}\right)A_1\left(r'\right)\right\}\times\frac{\partial i_{gr}\left(r',t-\frac{R(r')}{c}\right)}{\partial t}\\
&+\left\{\frac{A_1(r')A_2(r')\cos\theta-A_1\left(r'\right)^2\sin\theta}{2cR\left(r'\right)^4}+\frac{\sin\theta}{cR\left(r'\right)^2}\right\}\times\frac{\partial i_{gr}\left(r',t-\frac{R(r')}{c}\right)}{\partial t}\\
&-\frac{1}{2}\left\{\left(\frac{-A_2\left(r'\right)\cos\theta+A_1\left(r'\right)\sin\theta}{2c^2R\left(r'\right)^3}\right)A_1\left(r'\right)\right\}\times\frac{\partial {i_{gr}}^2\left(r',t-\frac{R(r')}{c}\right)}{\partial t^2}\\
&-\left\{\frac{3x^2\sin\theta}{R(r')^5}-\frac{\sin\theta}{R\left(r'\right)^3}\right\}\times i_{gr}\left(r',t-\frac{R\left(r'\right)}{c}\right)-\frac{x^2\sin\theta}{cR\left(r'\right)^4}\times\frac{\partial i_{gr}\left(r',t-\frac{R(r')}{c}\right)}{\partial t}\\
&\left.-\left\{\frac{2x^2\sin\theta}{cR(r')^4}-\frac{\sin\theta}{cR(r')^2}\right\}\times\frac{\partial i_{gr}\left(r',t-\frac{R(r')}{c}\right)}{\partial t}-\frac{x^2\sin\theta}{c^2R(r')^3}\times\frac{\partial {i_{gr}}^2\left(r',t-\frac{R(r')}{c}\right)}{\partial t^2}\right]\\
&F_{i,5}\left(x,y,z,\theta,t,r'\right)\\
&=\frac{1}{4\pi\varepsilon_0}\times\left[\left\{\frac{-3x^2\cos\theta}{R\left(r'\right)^5}+\frac{\cos\theta}{R\left(r'\right)^3}\right\}\times i_{gr}\left(r',t-\frac{R\left(r'\right)}{c}\right)-\frac{x^2\cos\theta}{cR\left(r'\right)^4}\right.\\
&\times\frac{\partial i_{gr}\left(r',t-\frac{R(r')}{c}\right)}{\partial t}+\left\{\frac{-2x^2\cos\theta}{cR\left(r'\right)^4}+\frac{\cos\theta}{cR\left(r'\right)^2}\right\}\times\frac{\partial i_{gr}\left(r',t-\frac{R(r')}{c}\right)}{\partial t}
\end{aligned}
$$

$$-\frac{x^2\cos\theta}{c^2R\left(r'\right)^3}\times\frac{\partial {i_{gr}}^2\left(r',t-\frac{R(r')}{c}\right)}{\partial t^2}-\left\{\frac{3A_2\left(r'\right)^2\cos\theta-3A_1\left(r'\right)A_2(r')\sin\theta}{4R\left(r'\right)^5}\right.$$
$$\left.-\frac{\cos\theta}{R(r')^3}\right\}\times i_{gr}\left(r',t-\frac{R\left(r'\right)}{c}\right)+\frac{1}{2}\left\{\left(\frac{-A_2\left(r'\right)\cos\theta+A_1\left(r'\right)\sin\theta}{2cR\left(r'\right)^4}\right)A_2\left(r'\right)\right\}$$
$$\times\frac{\partial i_{gr}\left(r',t-\frac{R(r')}{c}\right)}{\partial t}-\left\{\frac{A_2\left(r'\right)^2\cos\theta-A_1\left(r'\right)A_2\left(r'\right)\sin\theta}{2cR\left(r'\right)^4}-\frac{\cos\theta}{cR\left(r'\right)^2}\right\}$$
$$\times\frac{\partial i_{gr}\left(r',t-\frac{R(r')}{c}\right)}{\partial t}+\frac{1}{2}\left\{\left(\frac{-A_2\left(r'\right)\cos\theta+A_1\left(r'\right)\sin\theta}{2c^2R\left(r'\right)^3}\right)A_2\left(r'\right)\right\}$$
$$\times\frac{\partial {i_{gr}}^2\left(r',t-\frac{R(r')}{c}\right)}{\partial t^2}\Bigg]$$

$$\Delta h_i=\begin{cases}\dfrac{\beta\chi^2\left\{(ct_i-ct_{i-1})-\sqrt{(\beta ct_i-z)^2+\left(\frac{r}{x}\right)^2}-\sqrt{(\beta ct_{i-1}-z)^2+\left(\frac{r}{x}\right)^2}\right\}}{\cos\theta}\\ \beta\chi^2\left\{-(\beta z+ct_i)+\sqrt{(\beta ct_i-z)^2+\left(\dfrac{r}{x}\right)^2}\right\}\cos\theta\quad\text{for}\quad i=1\end{cases}$$

$$\Delta h_i'=\begin{cases}\dfrac{\beta\chi^2\left\{(ct_{i-1}-ct_i)+\sqrt{(\beta ct_i+z)^2+\left(\frac{r}{x}\right)^2}-\sqrt{(\beta ct_{i-1}+z)^2+\left(\frac{r}{x}\right)^2}\right\}}{\cos\theta}\\ \dfrac{\beta\chi^2\left\{-(\beta z+ct_i)+\sqrt{(\beta ct_i+z)^2+\left(\frac{r}{\chi}\right)^2}\right\}}{}\cos\theta\quad\text{for}\quad i=1\end{cases}$$

$$h_{m,i}=\begin{cases}\dfrac{(m-1)\times\Delta h_i}{k}+h_{m=k+1,i-1}\\ \dfrac{(m-1)\times\Delta h_i}{k}\quad\text{for}\quad i=1\end{cases}$$

$$h'_{m,i}=\begin{cases}\dfrac{(m-1)\times\Delta {h'}_i}{k}+h'_{m=k+1,i-1}\\ \dfrac{(m-1)\times\Delta {h'}_i}{k}\quad\text{for}\quad i=1\end{cases}$$

$$a_m=\begin{cases}\dfrac{\Delta h_i}{2\times k}\quad\text{for}\quad m=1\quad\text{and}\quad m=k+1\\ \dfrac{\Delta h_i}{k}\quad\text{for others}\end{cases}$$

$$a'_m = \begin{cases} \dfrac{\Delta h'_i}{2 \times k} & \text{for} \quad m = 1 \quad \text{and} \quad m = k+1 \\ \dfrac{\Delta h'_i}{k} & \text{for others} \end{cases}$$

$k$ is the division factor ($>= 2$),

Therefore, the electromagnetic fields due to an inclined lightning channel are strongly dependent on the channel angle, the angle of the observation point and the ground reflection factor as well as other current and geometrical parameters. Likewise, the proposed field expressions can consider a number of different current functions and current models directly in the time domain without the need to apply any extra conversions. It is observed that the values of the $F_{i,1}$, $F_{i,2}$, $F_{i,3}$, $F_{i,4}$ and $F_{i,5}$, terms in Equations (4) to (6) are zero at time periods less than or equal to $\frac{\sqrt{x^2+y^2+z^2}}{c}$. It should be mentioned that by selecting higher value of $k$ parameter, the accuracy of result can be increased. In this paper the values of $\Delta t$ and $k$ are set at 0.02 µs and 3, respectively with the corresponding average value of $\Delta h$ about 1.7 m whereas each step of Trapezoid considers on the effect of 0.6 m of channel on the field and the inherent error of Trapezoid in this scale can be neglected.

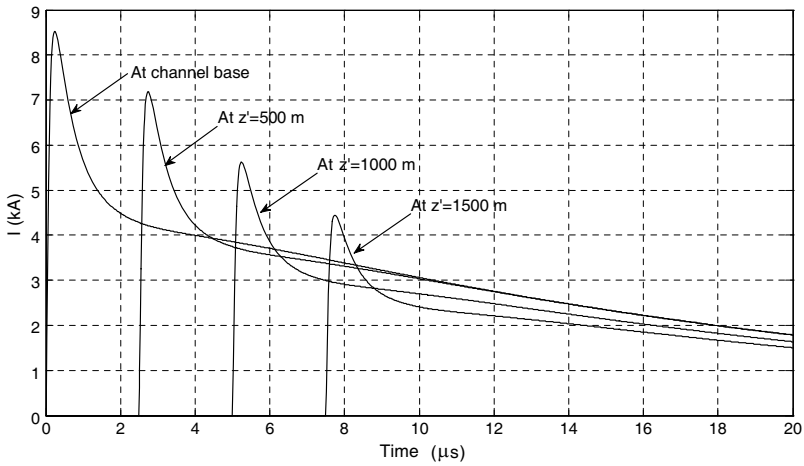


**Figure 2.** Simulated current wave shapes at different heights along lightning channel ($\lambda = 2000$ m, $\rho_g = 0.1$, $v = 2 \times 10^8$ m/s).

**Table 1.** The channel base current parameters based on Equation (1).

| $i_{01}$ (kA) | $i_{02}$ (kA) | $\tau_{11}$ (μs) | $\tau_{12}$ (μs) | $\tau_{21}$ (μs) | $\tau_{22}$ (μs) | $n_1$ | $n_2$ |
|---|---|---|---|---|---|---|---|
| 8 | 3.66 | 0.095 | 0.85 | 1.4 | 18 | 2 | 2 |

## 4. RESULTS AND DISCUSSION

In order to test the proposed field expressions with experimental data, a set of measured electromagnetic fields associated with an inclined lightning channel are used and the simulated fields are compared with the corresponding measured fields. It should be mentioned that the measured fields are obtained from a triggered lightning experiment based on the geometry of field sensors as illustrated in Figure 4 and the current parameters are as listed in Table 1 [6, 8, 28] as follows.

Figure 2 shows the current wave shapes at different heights along the lightning channel whereby the ground reflection factor is set to 0.1 and the current parameters are obtained from Table 1. The current model is set to the MTLE model with the values of $\lambda$ and $v$ equal to 2000 m and $2\times10^8$ m/s, respectively.

On the other hand, the behaviour of the current peak versus the ground reflection changes at two different channel heights as illustrated in Figure 3 which shows the current peak has a direct relationship with the value of the ground reflection factor.

Figure 5 shows the simulated magnetic flux densities based on different values of the ground reflection factors that are compared to the corresponding measured fields whereby the channel and the observation point angles are set to 20° and 45°, respectively. The results illustrate that the simulated fields based on $\rho_g = 0.1$ are in better agreement with the measured fields compared to other simulated fields while the peaks of the magnetic flux densities are directly dependent on the values of the ground reflection factor. It should be mentioned that in the experimental setup, the rocket launcher was located underground whereas a metal rod with the height about 2 m above ground surface was used as a striking object and the launcher and the rod were located at the center of a grounded area (with metal gird).

Moreover, Figure 6 shows a comparison between the simulated $\frac{dB_\phi}{dt}$ based on different values of ground reflection factors and the corresponding measured fields whereby the channel and the observation point angles are set at 20° and 120°, respectively. The results show that the simulated fields based on the values of the ground reflection

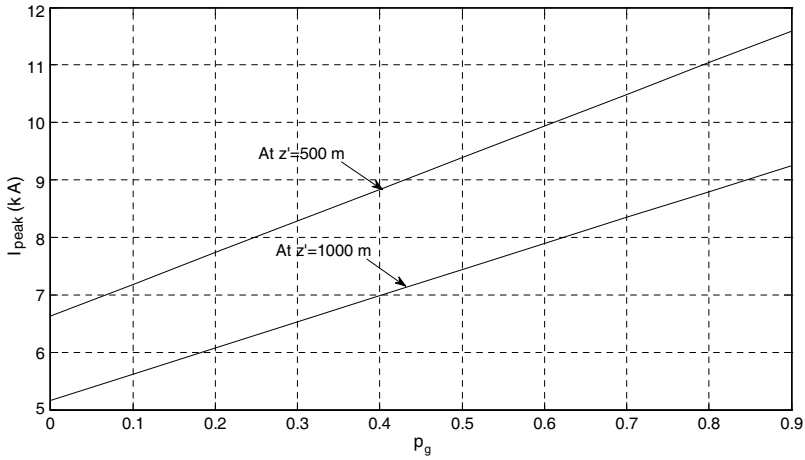


**Figure 3.** The behaviour of current peak versus ground reflection factor changes at two different levels along lightning channel ($\lambda = 2000\,\mathrm{m}$, $v = 2 \times 10^8\,\mathrm{m/s}$).

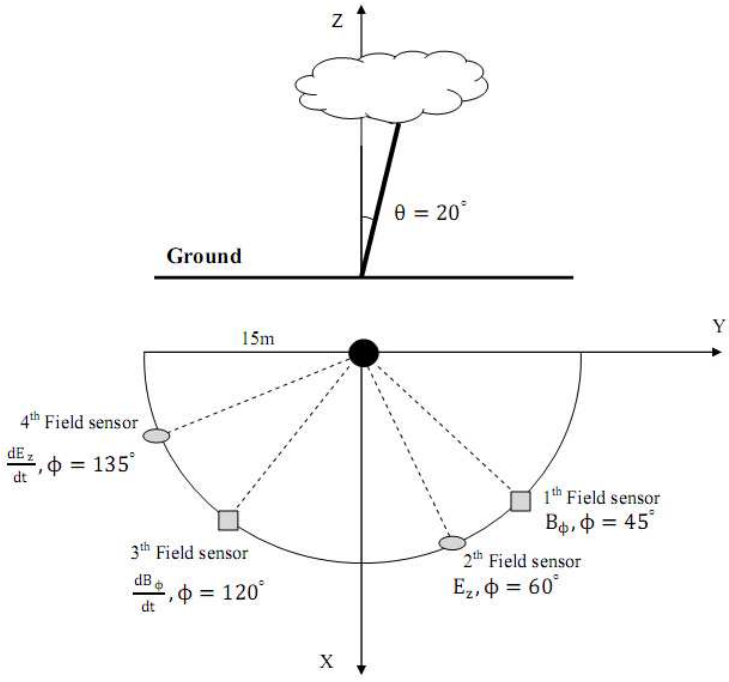


**Figure 4.** The geometry of field sensors.

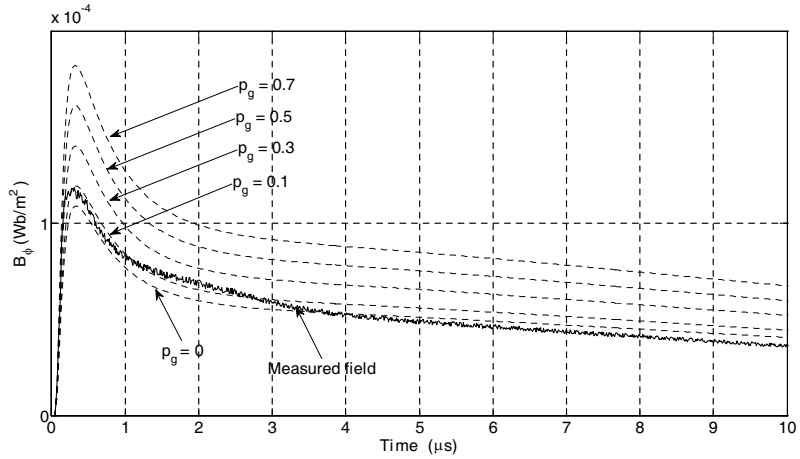


**Figure 5.** Comparison between simulated magnetic flux densities and corresponding measured field ($r = 15\,\mathrm{m}$, $z = 0$, $\theta = 20°$, $\phi = 45°$, $v = 2 \times 10^8\,\mathrm{m/s}$).

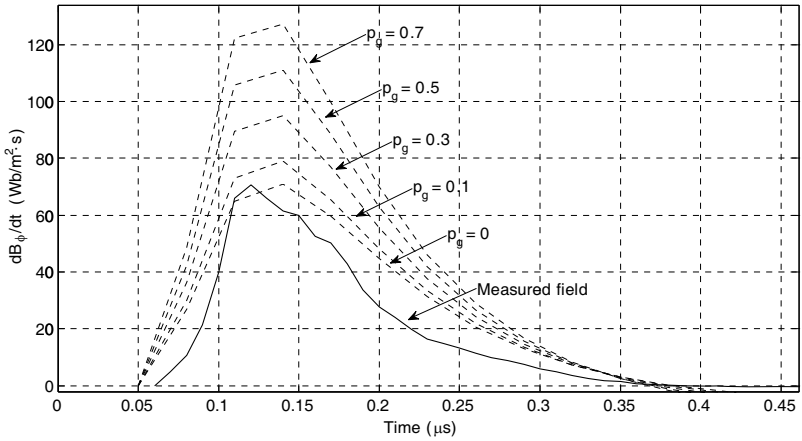


**Figure 6.** Comparison between simulated $\frac{dB_\phi}{dt}$ and corresponding measured field ($r = 15\,\mathrm{m}$, $z = 0$, $\theta = 20°$, $\phi = 120°$, $v = 2 \times 10^8\,\mathrm{m/s}$).

factors of 0 and 0.1 are in better agreement with the corresponding measured fields compared to the other simulated fields. By increasing the ground reflection factors the peaks of $\frac{dB_\phi}{dt}$ are increased.

Likewise, the simulated $\frac{dE_z}{dt}$ based on different values of ground reflection factors are compared to the corresponding measured fields

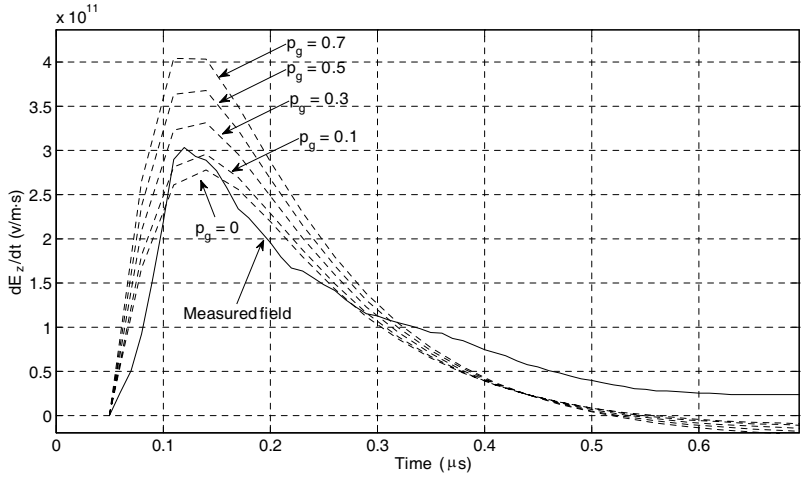


**Figure 7.** Comparison between simulated $\frac{dE_z}{dt}$ and corresponding measured field ($r = 15\,\text{m}$, $z = 0$, $\theta = 20^\circ$, $\phi = 135^\circ$, $v = 2 \times 10^8\,\text{m/s}$).

as shown in Figure 7 whereas the observation point is located at 135° with respect to the image of the lightning channel on the surface of the ground.

The results show that the simulated field based on $\rho_g = 0.1$ is in better agreement with the corresponding measured field compared to other simulated fields. Moreover, it illustrates that the ground reflection factor has a direct relationship with the peak of $\frac{dE_z}{dt}$. Figure 8 shows a comparison between the simulated vertical electric field based on different values of reflection factor and the corresponding measured field for which the observation point is set on the surface of the ground with the observation point angle equal to 60° with respect to the image of the lightning channel on the surface of the ground. The results show that the simulated field based on $\rho_g = 0.1$ is in good agreement with the corresponding measured field while the peaks of the simulated fields have a direct relationship with the values of the ground reflection factor. It should be mentioned that the difference between the simulated field (based on $\rho_g = 0.1$) and the corresponding measured field of that period can be due to inherent error of applied current model and also velocity profile along lightning channel, that is assumed as a constant value. In reality return stroke velocity is a height dependent variable [10, 19].

The effect of the observation point angle on the peak values of the electromagnetic fields are considered as shown in Figure 9 using a ground reflection factor of 0.1. The figure shows that the peak values of

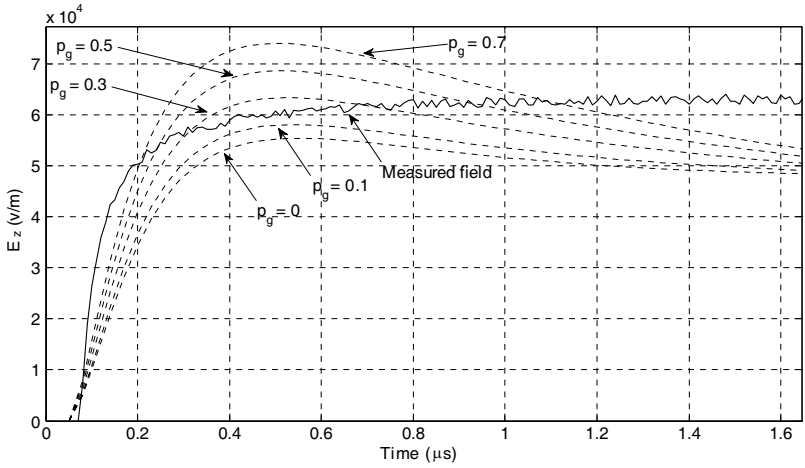


**Figure 8.** Comparison between simulated vertical electric fields and corresponding measured field ($r = 15\,\text{m}$, $z = 0$, $\theta = 20°$, $\phi = 60°$, $v = 2 \times 10^8\,\text{m/s}$).

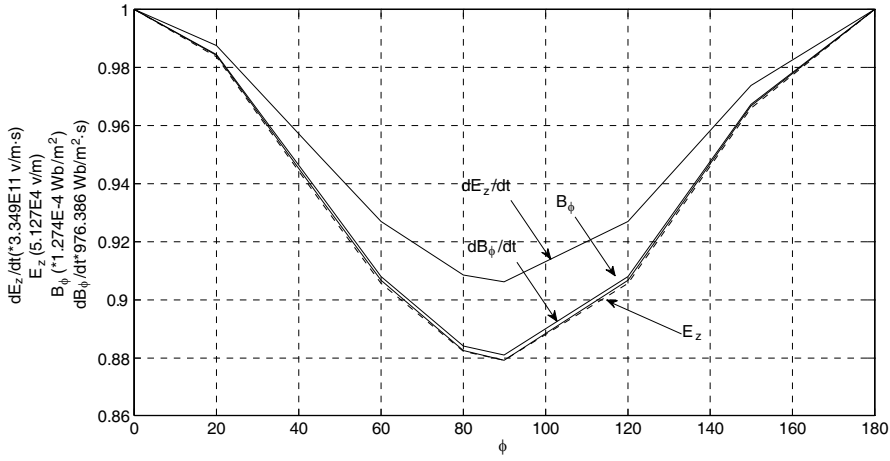


**Figure 9.** The behavior of field peaks versus observation point angle changes ($r = 15\,\text{m}$, $z = 0$, $\theta = 20°$, $\rho_g = 0.1$, $v = 2 \times 10^8\,\text{m/s}$).

the electromagnetic fields have a decreasing trend up to approximately $\phi = 90^\circ$ and after this angle the peak values show an increasing trend due to the change in the temporary radial distance with respect to the observation point at different observation point angles.

Likewise, the channel angle effect on the peak values of the electromagnetic fields at $\phi = 45^\circ$ is considered by Figure 10 whereby

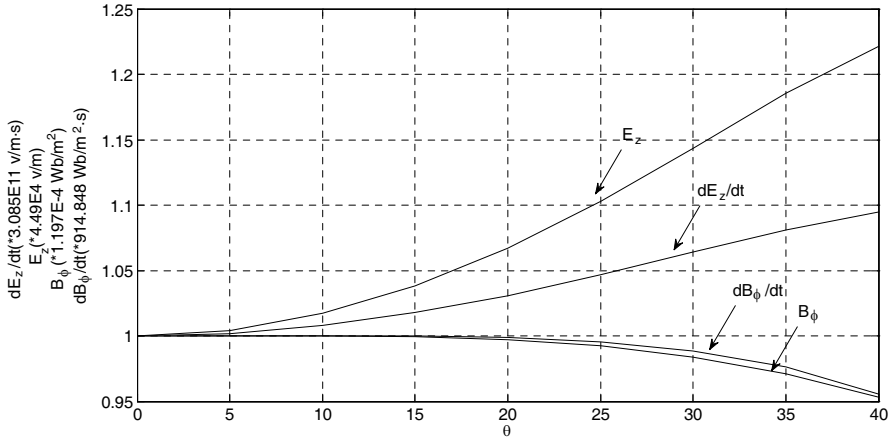


**Figure 10.** The behavior of field peaks versus channel angle changes ($r = 15\,\text{m}$, $z = 0$, $\phi = 45^\circ$, $\rho_g = 0.1$, $v = 2 \times 10^8\,\text{m/s}$).

the observation point is located on the surface of the ground and the ground reflection factor is set to 0.1.

Figure 10 shows that by increasing the channel angle with respect to the vertical axis, the peak values of the vertical electric fields and the derivative of the vertical electric field to time have a nonlinear increasing trend while the peak values of the magnetic flux densities and the derivative of the magnetic flux densities to time have an inverse relationship with the values of the channel angle. The proposed method can support different current functions and models directly in the time domain. Moreover, the proposed field expression can include the angle of the lightning channel with respect to vertical axis as well as the ground reflection at the striking point. The channel parameters and also the ground reflection factor have an effect on the values of the electromagnetic fields. It should be mentioned that in the coupling models the evaluated values of the lightning induced voltage on the power lines are directly dependent on the electromagnetic field components especially the vertical electric field component [29–32]. Therefore, determining the channel angle and the ground reflection factor can be useful for setting the appropriate protection level for power lines versus a lightning induced voltage.

## 5. CONCLUSION

In this paper, the electromagnetic fields due to an inclined lightning channel in the presence of a ground reflection factor are considered. The analytical field expressions due to an inclined channel are proposed

whereby they can support different current functions and models directly in the time domain and they can be combined with coupling models to set the appropriate protection level for the power lines by determining the channel parameters and the ground reflection. By using a set of measured fields from a triggered lightning experiment, the effects of the critical parameters on the values of the electromagnetic field are considered and the results discussed accordingly.

## REFERENCES

1. Andreotti, A., F. Mottola, M. Pagano, and L. Verolino, "Lightning induced voltages on power lines: A new statistical approach," *International Symposium on Power Electronics, Electrical Drives, Automation and Motion, SPEEDAM*, 445–451, 2008.
2. Ianoz, M., "Review of new developments in the modeling of lightning electromagnetic effects on overhead lines and buried cables," *IEEE Transactions on Electromagnetic Compatibility*, Vol. 49, 224–236, 2007.
3. Yang, C. and B. Zhou, "Calculation methods of electromagnetic fields very close to lightning," *IEEE Transactions on Electromagnetic Compatibility*, Vol. 46, 133–141, 2004.
4. Moini, R., S. Sadeghi, and B. Kordi, "An electromagnetic model of lightning return stroke channel using electric field integral equation in time domain," *Engineering Analysis With Boundary Elements*, Vol. 27, 305–314, 2003.
5. Izadi, M, M. Z. Ab Kadir, C. Gomes, and W. F. W. Ahmad, "An analytical second-fdtd method for evaluation of electric and magnetic fields at intermediate distances from lightning channel," *Progress In Electromagnetics Research*, Vol. 110, 329–352, 2010.
6. Izadi, M., M. Z. A. Ab Kadir, and C. Gomes, "Evaluation of electromagnetic fields associated with inclined lightning channel using second order FDTD-hybrid methods," *Progress In Electromagnetics Research*, Vol. 117, 209–236, 2011.
7. Izadi, M., A. Kadir, and A. Rahman, "On comparison between rusck and taylor coupling models for evaluation of lightning induced voltage on the power lines (⟨Special Issue⟩ *Asia-Pacific Symposium on Applied Electromagnetics and Mechanics (APSAEM10)*)," *Journal of the Japan Society of Applied Electromagnetics*, Vol. 19, S131–S134, 2011.
8. Izadi, M., M. Z. Ab Kadir, C. Gomes, and W. F. H. W. Ahmad, "Analytical expressions for electromagnetic fields associated with

the inclined lightning channels in the time domain," *Electric Power Components and Systems*, Vol. 40, 414–438, 2012.

9. Izadi, M., M. Z. Ab Kadir, C. Gomes, and W. Wan Ahmad, "Evaluation of electromagnetic fields due to lightning channel with respect to the striking angle," *International Review of Electrical Engineering (IREE)*, Vol. 6, 1013–1023, 2011.
10. Izadi, M., M. Z. A. Ab Kadir, C. Gomes, V. Cooray, and J. Shoene, "Evaluation of lightning current and velocity profiles along lightning channel using measured magnetic flux density," *Progress In Electromagnetics Research*, Vol. 130, 473–492, 2012.
11. Izadi, M., M. Z. A. Ab Kadir, C. Gomes, and V. Cooray, "Evaluation of lightning return stroke current using measured electromagnetic fields," *Progress In Electromagnetics Research*, Vol. 130, 581–600, 2012.
12. Vujević, S., D. Lovrić, and I. Jurić-Grgić, "Least squares estimation of Heidler function parameters," *European Transactions on Electrical Power*, Vol. 21, 329–344, 2011.
13. Heidler, F., "Analytische blitzstromfunktion zur LEMP-berechnung," *Presented at the 18th ICLP Munich*, Germany, 1985.
14. Izadi, M. and M. Kadir, "New algorithm for evaluation of electric fields due to indirect lightning strike," *CMES: Computer Modeling in Engineering & Sciences*, Vol. 67, 1–12, 2010.
15. Rakov, V., "Lightning electromagnetic fields: Modeling and measurements," *12th Int. Zurich Symposium on Electromagnetic Compatibility*, 59–64, Zurich, Switzerland, 1997.
16. Cooray, V., *The Lightning Flash*, IET Press, 2003.
17. Izadi, M, M. Z. A. Kadir, C. Gomes, and M. T. Askari, "Evaluation of lightning return stroke parameters using measured magnetic flux density and PSO algorithm," *Przegląd Elektrotechniczny (Electrical Review)*, Vol. R. 88, NR 10a, 2012.
18. Nucci, C. A., "Lightning-induced voltages on overhead power lines. Part I: Return stroke current models with specified channel-base current for the evaluation of the return stroke electromagnetic fields," *Electra*, Vol. 161, 75–102, 1995.
19. Rakov, V., "Lightning return stroke speed," *Journal of Lightning Research*, Vol. 1, 2007.
20. Bermudez, J. L., "Lightning currents and electromagnetic fields associated with return strokes to evaluated strike objects," Ph.D. Ecole Polytechnique Federale De Lausanne, 2003.
21. Zhou, X., "On independence completeness of Maxwell's equations and uniqueness theorems in electromagnetics," *Progress In*

*Electromagnetics Research*, Vol. 64, 117–134, 2006.

22. Chen, J. and Q. Liu, "A non-spurious vector spectral element method for Maxwell's equations," *Progress In Electromagnetics Research*, Vol. 96, 205–215, 2009.
23. Nevels, R. and C. S. Shin, "Lorenz, lorentz, and the gauge," *IEEE Antennas & Propagation Magazine*, Vol. 43, 70–72, 2001.
24. Thottappillil, R. and V. Rakov, "Review of three equivalent approaches for computing electromagnetic fields from an extending lightning discharge," *Journal of Lightning Research*, Vol. 1, 90–110, 2007.
25. Izadi, M., M. Z. A. A. Kadir, C. Gomes, and W. F. W. Ahmad, "Numerical expressions in time domain for electromagnetic fields due to lightning channels," *International Journal of Applied Electromagnetics and Mechanics*, Vol. 37, 275–289, 2011.
26. Kreyszig, E., *Advanced Engineering Mathematics*, Wiley-India, 2007.
27. Matthew, N. O. S., *Numerical Technique in Electromagnetics*, CRC Press, LLC, 2001.
28. Kodali, V., V. Rakov, M. Uman, K. Rambo, G. Schnetzer, J. Schoene, and J. Jerauld, "Triggered-lightning properties inferred from measured currents and very close electric fields," *Atmospheric Research*, Vol. 76, 355–376, 2005.
29. Paolone, M., C. Nucci, E. Petrache, and F. Rachidi, "Mitigation of lightning-induced overvoltages in medium voltage distribution lines by means of periodical grounding of shielding wires and of surge arresters: Modeling and experimental validation," *IEEE Transactions on Power Delivery*, Vol. 19, 423–431, 2004.
30. Paolone, M., C. Nucci, and F. Rachidi, "A new finite difference time domain scheme for the evaluation of lightning induced overvoltage on multiconductor overhead lines," *International Conference on Power System Transient (IPST)*, 596–602, 2001.
31. Nucci, C. A., "Lightning-induced voltages on overhead power lines. Part II: Coupling models for the evaluation of the induced voltages," *Electra*, Vol. 162, 121–145, 1995.
32. Nucci, C. A., F. Rachidi, M. Ianoz, and C. Mazzetti, "Comparison of two coupling models for lightning-induced overvoltage calculations," *IEEE Transactions on Power Delivery*, Vol. 10, 330–339, 1995.